

Dynamic Micellar Electrokinetic Chromatography. Determination of the Enantiomerization Barriers of Oxazepam, Temazepam, and Lorazepam

Gabriele Schoetz, Oliver Trapp, and Volker Schurig*

Universität Tübingen, Institut für Organische Chemie, Auf der Morgenstelle 18, 72076 Tübingen, Germany

The temperature-dependent enantiomerization barriers of oxazepam, temazepam, and lorazepam have been determined between 0 and 30 °C by dynamic micellar electrokinetic chromatography (DMEKC) in an aqueous 20 mM borate/phosphate buffer system at pH 8 with 60 mM sodium cholate as chiral surfactant. Interconversion profiles featuring plateau formation and peak broadening were observed and simulated by the new program ChromWin based on the theoretical plate as well as on the stochastic model using the experimental data plateau height, h_{plateau} , peak width at half-height, w_h , total retention times, t_R , and electroosmotic breakthrough time, t_0 . Peak form analysis yielded rate constants k and kinetic activation parameters, ΔG^\ddagger , ΔH^\ddagger , and ΔS^\ddagger , of the enantiomerization of oxazepam, temazepam, and lorazepam. At 25 °C, the enantiomerization barrier, ΔG^\ddagger , was determined to be ~ 90 kJ mol⁻¹ and the half-lives, τ , were determined to be approximately 21 min. The new approach allows the fast and precise determination of enantiomerization barriers in a biogenic environment and it mimics physiological conditions, as no organic modifiers or abiotic chiral stationary phases (CSP) are employed.

Policy statements of regulatory authorities such as the American Food and Drug Administration (FDA) not only restrict the sale of racemic drugs but demand unambiguous data on the configurational stability of pure enantiomers. Consequently, drug manufacturers are bound to assess the “stereochemical integrity” of enantiomers and to examine the “potential for interconversion...of the individual isomers”.^{1,2}

Enantiomerization, in contrast to racemization, constitutes a reversible first-order reaction.³ It arises from the interconversion of a stereogenic element in a particular molecule. Evaluation of the stereochemical integrity of chiral compounds can be achieved, inter alia, by employing enantioselective chromatography on chiral stationary phases (CSPs),⁴ a technique which is generally used for the determination of enantiomeric ratios. *Dynamic chroma-*

tography is defined as a method to study reversible interconversion processes proceeding during the time scale of partitioning, and it has previously been applied for the determination of enantiomerization barriers.^{5–17} In enantioselective chromatography, peak profiles such as plateau formation or peak broadening are occasionally observed. This phenomenon is sometimes considered as a complication of the separation process, and the undesired peak shapes are suppressed by the addition of organic modifiers or a change of the chiral stationary phase (CSP).¹⁸ Yet in dynamic chromatography, the characteristic peak profiles not only represent a diagnostic tool for an interconversion process itself, but are the prerequisite for the quantitative determination of enantiomerization barriers.

Dynamic chromatography allows the measurement of barriers above 80 kJ mol⁻¹ in a short time. In contrast to classical enantiomerization experiments (chiroptical methods), which require large quantities of single or enriched enantiomers, the determination of enantiomerization barriers by dynamic chromatography can be performed with minute amounts of the racemic sample. An indispensable requirement for the application of this method is the quantitative on-column separation of the enantiomers, whereby the interconversion process takes place in a chiral environment.⁵ Enantiomerization leads to peak broadening, plateau formation, and eventually peak coalescence, depending on the stereochemical lability of the chiral compound investigated. The shape of the chromatogram of the resolved racemate is therefore subject to the rate of interconversion of the two enantiomers and the chromatographic time scale of enantioseparation. Depending

- (5) Bürkle, W.; Karfunkel, H.; Schurig, V. *J. Chromatogr.* **1984**, *288*, 1–14.
- (6) Jung, M.; Schurig, V. *J. Am. Chem. Soc.* **1992**, *114*, 529–534.
- (7) Trapp, O.; Schurig, V. *J. Am. Chem. Soc.* **2000**, 1424–1430.
- (8) Wolf, C.; König, W. A.; Roussel, C. *Liebigs Ann. Chem.* **1994**, 781–786.
- (9) Wolf, C.; Pirkle, W. H.; Welch, C. J.; Hochmuth, D. H.; König, W. A.; Chee, G.-L.; Charlton, J. L. *J. Org. Chem.* **1997**, *62*, 5208–5210.
- (10) Mannschreck, A.; Zinner, H.; Pustet, N. *Chimia* **1989**, *43*, 165–166.
- (11) Veciana, J. I.; Crespo, M. *Angew. Chem., Int. Ed. Engl.* **1991**, *30*, 54–77.
- (12) Cabrera, K.; Jung, M.; Fluck, M.; Schurig, V. *J. Chromatogr., A.* **1996**, *731*, 315–321.
- (13) Friary, R. J.; Spangler, M.; Osterman, R.; Schulman, L.; Schwerdt, J. H. *Chirality* **1996**, *8*, 364–371.
- (14) Gasparrini, F.; Misiti, D.; Pierini, M.; Villani, C. *Tetrahedron: Asymmetry* **1997**, *8*, 2069–2073.
- (15) Oxelbark, J.; Allenmark, S. *J. Org. Chem.* **1999**, *64*, 1483–1486.
- (16) Jung, M. Program Simul, No. 620, Quantum Chemistry Program Exchange. *QCPE Bull.* **1992**, *3*, 12.
- (17) Schoetz, G.; Trapp, O.; Schurig, V. *Enantiomer*, accepted for publication.
- (18) Boonkerd, S.; Detaevnier, M. R.; Michotte, Y.; Vindevogel, J. *J. Chromatogr., A* **1995**, *704*, 238–241.

* Corresponding author: Phone: +49-7071-2976257. Fax: +49-7071-295538. e-mail: volker.schurig@uni-tuebingen.de

(1) FDA. *Chirality* **1992**, *4*, 338–340.

(2) De Camp, W. H. *Chirality* **1989**, *1*, 2–6.

(3) Reist, M.; Testa, B.; Carrupt, P. A.; Jung, M.; Schurig, V. *Chirality* **1995**, *7*, 396–400.

(4) Schurig, V.; Bürkle, W. *J. Am. Chem. Soc.* **1982**, *104*, 7573–7580.

on the enantiomerization temperature, different chromatographic techniques (e.g., DGC, DHPLC, DMEKC) may be applied for the quantification of the enantiomerization process at a given time and temperature.

By comparison of experimental and computer-simulated chromatograms, kinetic activation parameters (ΔH^\ddagger and ΔS^\ddagger) of enantiomerization are obtained. The first simulation program was published in 1984⁵ and based on the theoretical plate model; later it was extended to simulations of up to 120 000 effective plates (SIMUL).^{6,16} The stochastic model,^{19–21} which treats peaks as a Gaussian curve and utilizes a probability distribution to describe the interconverting species of the enantiomers, has also been applied for the determination of enantiomerization barriers.^{10,11} The new program ChromWin²² allows simulation with the theoretical plate model, the stochastic model, and a modified stochastic model and is running on a personal computer under Windows. It allows the simulation of chromatograms with large plate numbers usually obtained by capillary gas chromatography and capillary electromigration methods.

In the present study, dynamic micellar electrokinetic chromatography (DMEKC) was applied to determine the enantiomerization barrier of the chiral benzodiazepine drugs oxazepam, temazepam, and lorazepam in a single-phase system whereby the chiral surfactant is dissolved in the running buffer. The enantiomerization barriers were determined by comparing elution profiles obtained experimentally by DMEKC in the presence of sodium cholate with elution profiles simulated with the ChromWin program. The present examples were selected (i) to show the applicability of DMEKC as a general method for the determination of enantiomerization barriers, (ii) to demonstrate the efficiency of the simulation program at large plate numbers, and (iii) to prove the applicability of both the theoretical plate model and the stochastic model to one-phase systems involving chromatographic partitioning in the presence of micelles (MEKC).

EXPERIMENTAL SECTION

Materials. The tranquilizers, oxazepam, temazepam, lorazepam, and the sodium phosphate (NaH_2PO_4 99%) and sodium borate ($\text{Na}_2\text{B}_4\text{O}_7 \cdot 10 \text{H}_2\text{O}$ 99%) buffer salts were purchased from Sigma-Aldrich (Deisenhofen, Germany). The sodium salt of $3\alpha,7\alpha,12\alpha$ -trihydroxy- 5β -cholic-acid (purum) was obtained from Fluka (Buchs, Switzerland). One molar HPLC grade sodium hydroxide solution (E. Merck, Darmstadt, Germany) was diluted with 18.2 M Ω high purity water obtained from a Millipore-Q System (Millipore, Marlborough, Massachusetts). High-purity water, 18.2 M Ω , was also used to prepare the borate and phosphate buffer solutions. All benzodiazepine samples were dissolved in HPLC-grade methanol (E. Merck, Darmstadt, Germany), and the concentration was adjusted to 0.1 mg/mL. Before use, all sample and buffer solutions were passed through a 0.45- μm disposable filter cartridge (Chromafil, Machery and Nagel, Düren, Germany).

Capillary Electrophoresis. The separation of the enantiomers of the three benzodiazepines was carried out with a Prince Unicam Crystal 300/31 capillary electrophoresis system equipped with an

on-column UV detector (Bischoff Lamda 1000, Leonberg, Germany) and a thermostated homemade water cooling system with integrated temperature control (Haake D8-GH, Haake, Karlsruhe, Germany). The effective length of the fused silica capillary (Microquartz, Munich, Germany) was 95 cm (total length 112), the temperature-regulated length was 76 cm, and the inner diameter was 50 μm . Unless otherwise stated, 60 mM sodium cholate (SC), as a chiral surfactant, introduced by Terabe et al.,^{18,23–26} was used dissolved in 20 mM borate/phosphate buffer solution at a pH of 8. The temperature of the thermostated zone ranged from 0 to 30 °C. UV detection was performed at 230 nm. Peak integration was carried out with a Chromopak C-R6A integrator (Shimadzu, Kyoto, Japan).

Untreated silica capillaries were conditioned for 30 min with 0.1 M NaOH solution. Afterward, the capillary was purged with running buffer for 30 min. Between injections, the capillary was rinsed with running buffer for 5 min. Before any change of analyte or buffer concentration, the capillary was treated with 0.1 M NaOH solution for 10 min, followed by running buffer for 30 min. Injections were performed hydrodynamically at the anodic side by applying a pressure of 20 mbar for two seconds. A voltage of +25 kV was used for separation.

Computer Simulation. For the calculation of the enantiomerization barrier, the plateau height, h_{plateau} ; peak width at half-height, w_h ; total retention times, t_R , of the enantiomers; and the electroosmotic break through time, t_0 , (using dimethylformamide as a marker) of the experimental chromatograms were used. Since the peak profiles of interconverting enantiomers are broadened (tailing of the first eluted enantiomer and fronting of the second eluted enantiomer), plate numbers have to be adjusted for simulation to fit the experimental chromatogram. While the use of effective plate numbers, N_{eff} , in the simulation leads to peak widths of the simulated chromatogram that are too large, the use of the theoretical plate numbers, N_{th} , leads to peak widths that are too small. Therefore, as a compromise, mean plate numbers \bar{N} , calculated from the modified eq 1,¹⁵ were applied. This equation, established for gas-chromatographic two-phase systems,¹⁶ can be adopted here because of the long retention time of the micellar pseudo stationary phase (using Sudan III as a marker) and the relative insensitivity of the simulation program toward errors in plate numbers, N .

$$\bar{N} = 5.545 \frac{t_R(t_R - t_M)}{(w_h)^2} \quad (1)$$

The initially injected amounts of the enantiomers were set equal for the racemic benzodiazepine samples. Peak form analysis was performed with ChromWin according to the theoretical plate model and the modified stochastic model using an improved Newton algorithm in order to find the best agreement of the simulated and experimental elution profiles in only a few simulation steps. The program furnishes the apparent rate constants,

(19) Keller, R. A.; Giddings, J. C. *J. Chromatogr.* **1960**, *3*, 205–220.

(20) Kramer, R. *J. Chromatogr.* **1975**, *107*, 241–252.

(21) Cremer, E.; Kramer, R. *J. Chromatogr.* **1975**, *107*, 253–263.

(22) Trapp, O.; Schurig, V. *Comput. Chem.* **2000**, *24*, in press. Information available from the authors upon request.

(23) Terabe, S.; Otsuka, K.; Ando, T. *Anal. Chem.* **1985**, *57*, 834–841.

(24) Terabe, S.; Shibata, M.; Miyashita, Y. *J. Chromatogr., A* **1989**, *480*, 403–411.

(25) Otsuka, K.; Terabe, S. *J. Chromatogr., A* **1990**, *515*, 221–226.

(26) Muijselaar, P. G.; Otsuka, K.; Terabe, S. *J. Chromatogr., A* **1997**, *780*, 41–61.

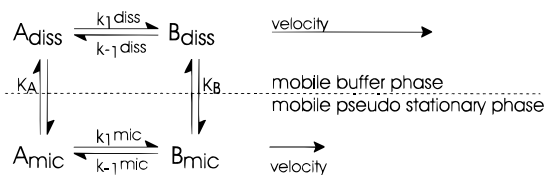


Figure 1. Principle of microscopic reversibility. Equilibria in a theoretical plate: A is the first eluted enantiomer, B is the second eluted enantiomer, k represents the rate constant, and K represents the distribution constant.

k_1^{app} and k_{-1}^{app} , of enantiomerization in the presence of the chiral micelle. k_{-1}^{app} was calculated via eq 2 from k_1^{app} according to the principle of microscopic reversibility^{3,5} shown in Figure 1. The apparent rate constants, k_1^{app} and k_{-1}^{app} , arise from the rate constant k^{diss} in the dissolved state and k^{mic} in the micellar state according to eqs 3 and 4. The retention factors K_A of the first eluted enantiomer A and K_B of the second eluted enantiomer B have been calculated from the total retention time t_R and the electroosmotic break through time t_0 according to $K = (t_R - t_0)/t_0$.

$$\frac{k_1^{\text{app}}}{k_{-1}^{\text{app}}} = \frac{K_B}{K_A} \quad (2)$$

$$k_1^{\text{app}} = \frac{1}{1 + K_A} k^{\text{dis}} + \frac{K_A}{1 + K_A} k_1^{\text{mic}} \quad (3)$$

$$k_{-1}^{\text{app}} = \frac{1}{1 + K_B} k^{\text{dis}} + \frac{K_B}{1 + K_B} k_{-1}^{\text{mic}} \quad (4)$$

The apparent rate constants were evaluated from as many as 187 chromatograms. As the process of enantiomerization is defined as a reversible first-order microscopic process with $2k_{\text{enant}} = k_{\text{rac}}$, a statistical transmission factor, κ , of 0.5 was used in calculating the Gibbs activation energy, $\Delta G^\ddagger(T)$,^{3,12} from the rate constant k_1^{app} according to the Eyring equation, eq 5.

Enantiomerization studies were performed at different temperatures. According to the Gibbs–Helmholtz equation, $\Delta G^\ddagger(T) = \Delta H^\ddagger - T\Delta S^\ddagger$, the activation enthalpy, ΔH^\ddagger , was obtained via the slope and the activation entropy, ΔS^\ddagger , via the intercept of the Eyring plot (T^{-1} versus $\ln(k^{\text{app}}/T)$).

$$\Delta G(T) = -RT \ln \left(\frac{k_1^{\text{app}}}{\kappa} \frac{h}{k_B T} \right) \quad (5)$$

with κ as the transmission factor ($\kappa = 0.5$), k_B as the Boltzmann constant ($k_B = 1.380662 \times 10^{-23} \text{ J}\cdot\text{K}^{-1}$), T as the enantiomerization temperature [K], h as Planck's constant ($h = 6.626176 \times 10^{-34} \text{ J}\cdot\text{s}$), and R as the gas constant ($R = 8.31441 \text{ J}\cdot\text{K}^{-1}\cdot\text{mol}^{-1}$).

RESULTS

Temperature Regulation. To conduct reliable kinetic studies, precise control of the temperature is mandatory. Temperature control in capillary electrophoresis is difficult because of the strong internal Joule heating within the capillary, which influences the mobility of the analytes and the reproducibility of the separation.

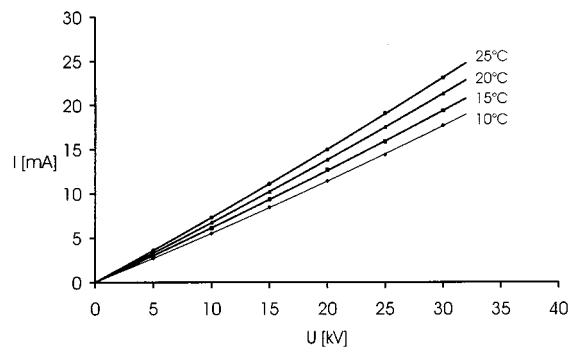


Figure 2. Ohm's Law plot at temperatures from 10 to 25 °C of a 60 mM borate/phosphate buffer solution at pH 8.

Internal Joule heating also leads to peak broadening, loss in resolution, and random enantiomerization of the enantiomers. Therefore, to gain temperature constancy, low ionic strength running buffers, small inner diameters of the capillaries, and low voltages may be used. However, despite the fact that all of these steps lead to a reduction in Joule heat, they do so at the expense of longer running times, increased peak broadening, decreased sensitivity, and lower resolution. Another strategy to reduce the side effects of Joule heating is an effective external cooling system. A standard air-ventilated system can hardly cope with the excessive heat generated within the capillary; this frequently causes temperature fluctuations, especially at higher buffer concentrations. Even commercial liquid cooled systems²⁷ cannot entirely compensate for heating effects, because the heat is not dissipated rapidly enough or the heat capacity of the coolant is too low. Water cooled systems, which have a larger heat capacity, are usually avoided in CE, because of the risk of a capillary breaking at high voltages.

In the present study a very effective and inexpensive homemade aqueous cooling system was used in order to perform reliable temperature-dependent measurements. The hazard of accidental capillary breaking was minimized by coating the outer wall of the fused silica capillary with nonconductive PTFE before inserting it into a water-filled PE tube which was connected to the thermostat. Because of the high pump efficiency (12 L/min), the generated heat was removed instantaneously. As a result, the resolution factor, R_s , of the separations increased and the enantiomerization conditions remained stable and reproducible as compared with those of the conventional methodology.

Evaluation of the efficacy of the developed cooling system was performed by the Ohm's Law relationship. Linearity in the Ohm plot is only achieved at a constant resistance. As Joule heating increases resistance, the current will deviate from linearity at increased voltage. Figure 2 shows highly linear Ohm plots (Figure 2, agreement factor > 0.9999) at different temperatures for a 60 mM borate/phosphate buffer solution at pH 8, thus indicating the absence of Joule heating in the thermostated system. The current was measured 5 min after the voltage was applied. Following each measurement, the capillary was flushed with buffer solution for 5 min at 1 bar. The temperature of the buffer solution was adjusted to 20 °C for all experiments.

Optimization of Surfactant and Buffer Concentrations. To optimize conditions of enantiomer separation, various buffer and

(27) Palmieri, R. H. Technical information T-1823-A; Beckman Instruments: Fullerton, California, USA 1996.

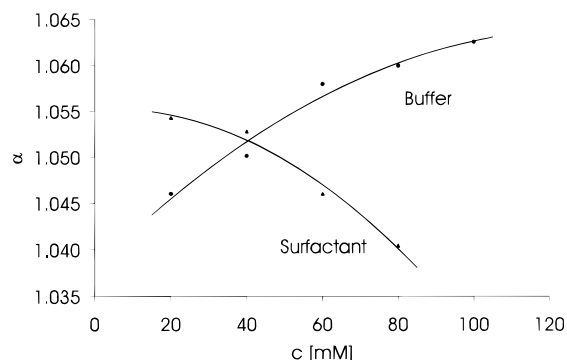


Figure 3. Concentration dependency of the separation factor α of the enantiomer separation of oxazepam. Chiral surfactant: sodium cholate. Buffer: borate/phosphate at pH 8. Column: 95 cm \times 50 μ m (i. d.). $U = 25$ kV. $\lambda = 230$ nm. $T = 10$ $^{\circ}$ C.

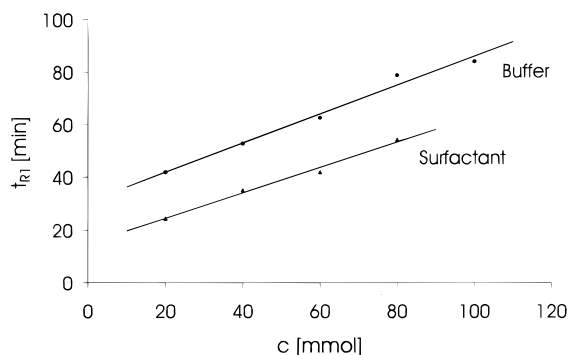


Figure 4. Concentration dependency of retention times, t_R , of the enantiomer separation of oxazepam. Chiral surfactant: sodium cholate. Buffer: borate/phosphate at pH 8. Column: 95 cm \times 50 μ m (i. d.). $U = 25$ kV. $\lambda = 230$ nm. $T = 10$ $^{\circ}$ C.

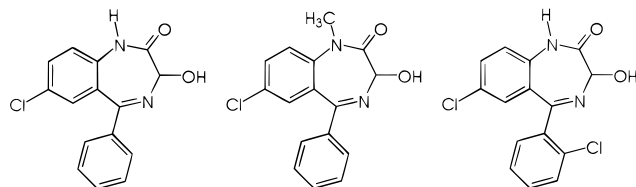


Figure 5. Structural formulas of the investigated benzodiazepines. From left to right: oxazepam, temazepam, and lorazepam.

surfactant concentrations were examined. Figure 3 shows the variation of buffer concentrations (borate/phosphate, pH 8), at a constant surfactant concentration (sodium cholate, SC) of 60 mM and for increasing SC concentrations at a buffer concentration of 20 mM. Whereas increase in buffer concentration leads to an increase in the separation factor α , a higher surfactant concentration results in a deterioration of the separation process. The optimum separation conditions were achieved at low surfactant and high buffer concentrations.

The concentration dependency of the retention times is shown in Figure 4. Elevated concentrations of buffer and surfactant lead to increasing retention times, whereby the rising buffer concentration shows a larger effect.

Finally, a buffer concentration of 20 mM and a surfactant concentration of 60 mM were chosen as a compromise between long retention times and a satisfactory enantiomer separation.

Enantiomerization. According to Figures 6 and 7, enantiomerization of oxazepam, temazepam, and lorazepam is recognized by characteristic plateau formation between 5 and 25 $^{\circ}$ C.

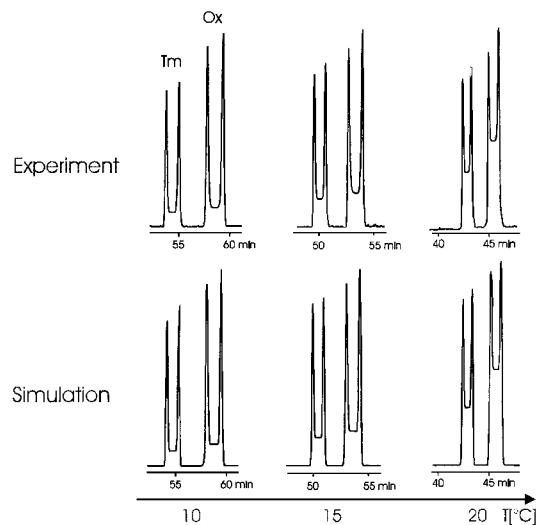


Figure 6. Experimental and simulated chromatograms of the simultaneous enantiomer separation of temazepam (Tm, left) and oxazepam (Ox, right) at different temperatures by DMEKC. Chiral surfactant: 60 mM sodium cholate. Buffer: 60 mM borate/phosphate at pH 8. Column: 95 cm \times 50 μ m (i. d.). $U = 25$ kV. $\lambda = 230$ nm.

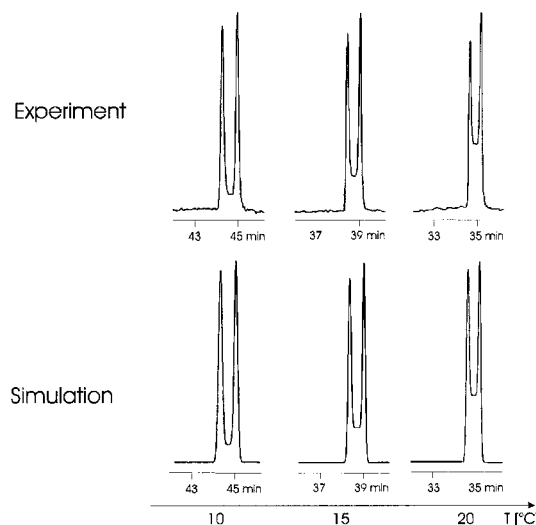


Figure 7. Experimental and simulated chromatograms of the simultaneous enantiomer separation of lorazepam at different temperatures by DMEKC. Chiral surfactant: 60 mM sodium cholate. Buffer: 20mM borate/phosphate at pH 8. Column: 95 cm \times 50 μ m (i. d.). $U = 25$ kV. $\lambda = 230$ nm.

The plateau arises from molecules which interconvert during the chromatographic time scale. For all investigated benzodiazepines (cf. Figure 5), peak coalescence commences at 30 $^{\circ}$ C, and a single broadened peak is observed for the enantiomers, whereas below 0 $^{\circ}$ C the usual baseline separation occurs. Chromatograms measured at these borderline temperatures were not utilized for computer simulation.

Computer Simulation. The chromatograms were simulated both with the theoretical plate model¹⁶ and the modified stochastic model of ChromWin using the experimental data plateau height, h_{plateau} ; peak width at half-height, $w_{1/2}$; total retention times, t_R , and electroosmotic break through time, t_0 . Kinetic activation data of enantiomerization were obtained by peak form analysis and iterative comparison of experimental and simulated chromatograms. The application of the principle of microscopic reversibility⁴

Table 1. Selected Experimental Data and Calculated Rate Constants of the Enantiomerizations of Oxazepam, Temazepam, and Lorazepam Obtained by ChromWin on the Basis of the Modified Stochastic Model¹⁶

no.	compound	T [°C]	t_{R1}	t_{R2}	\bar{N}_1	\bar{N}_2	$h_{\text{plateau}}[\%]$	k_1^{app}	k_{-1}^{app}
1	oxazepam	10	57.8	59.4	179 000	225 000	15	1.12×10^{-4}	1.07×10^{-4}
2	oxazepam	15	52.9	54.3	192 000	248 000	25	2.05×10^{-4}	1.79×10^{-4}
3	oxazepam	20	45.7	46.7	190 000	221 000	44	3.29×10^{-4}	3.15×10^{-4}
4	temazepam	10	53.2	54.5	157 000	149 000	11	7.30×10^{-5}	6.94×10^{-5}
5	temazepam	15	49.6	50.7	225 000	240 000	18	1.48×10^{-4}	1.41×10^{-4}
6	temazepam	20	43.2	44.1	280 000	320 000	34	3.05×10^{-4}	2.92×10^{-4}
7	lorazepam	10	44.5	45.1	209 000	241 000	9	9.64×10^{-5}	7.38×10^{-5}
8	lorazepam	15	38.4	39.0	214 000	268 000	25	1.86×10^{-4}	1.80×10^{-4}
9	lorazepam	20	34.7	35.2	236 000	270 000	42	3.07×10^{-4}	2.97×10^{-4}

Table 2. Kinetic Activation Parameters of the Enantiomerization of Oxazepam, Temazepam, and Lorazepam at 293 K and pH 8

compound	ΔG^\ddagger [kJ mol ⁻¹]	ΔH^\ddagger [kJ mol ⁻¹]	ΔS^\ddagger [J (K mol) ⁻¹]	k_f^{app} [10 ⁻⁴ s ⁻¹]	$t_{1/2}$ [min]
oxazepam	91.3 ± 0.1	72.0 ± 0.5	-65.8 ± 9	3.3	34.9
temazepam	91.6 ± 0.2	90.5 ± 0.7	-3.9 ± 12	2.9	39.8
lorazepam	91.4 ± 0.1	76.5 ± 0.6	-50.9 ± 8	3.1	37.3

Table 3. Results of Kinetic Activation Barriers of Independent Studies

compound	method/conditions	T [K]	ΔG^\ddagger [kJ mol ⁻¹]	k_f^{app} [10 ⁻⁴ s ⁻¹]	$t_{1/2}$ [min]	ref
oxazepam	DHPLC/ methanol/ phosphate buffer/pH 2.8	298	89.0			11
oxazepam	ethanolysis/ CD spectropolarimetry	298	92.1		11.8 ± 0.2	30
oxazepam	racemization/HPLC	273		0.268	~ 430	32
oxazepam	ethanolysis/HPLC/ 0.1 M H ₂ SO ₄	298	94.6		55.5 ± 0.2	35
temazepam	ethanolysis/ CD spectropolarimetry	298	95.0		38.6 ± 0.3	30
temazepam	ethanolysis/HPLC/ CD spectropolarimetry/ 0.5 M H ₂ SO ₄	298	90.8		12.7 ± 0.3	34
lorazepam	ethanolysis/HPLC	298			16.8 ± 0.8	28

requires that the rate constants of interconversion of the two enantiomers are different in the presence of the chiral surfactant. Thus, whereas the second eluted enantiomer is enriched at the chromatographic time scale as it is formed more rapidly than the first eluted enantiomer ($k_1^{\text{app}} > k_{-1}^{\text{app}}$), no overall deracemization occurs because the second enantiomer is depleted to a greater extent due to its longer residence time in the column. Examples for the experimental data used for the simulations are depicted in Table 1. The apparent rate constants obtained from the simulation are displayed graphically as an Eyring plot (Figure 8, agreement factor > 0.993). From the slope of this graph, the kinetic activation parameters given in Table 2 are obtained. The errors for the activation parameters ΔH^\ddagger and ΔS^\ddagger were determined from the standard deviations due to equations given by Sandström.²⁸

It is noteworthy that the values for ΔG^\ddagger of oxazepam, temazepam, and lorazepam are comparable to each other, whereas the ΔH^\ddagger and ΔS^\ddagger values are different. The better agreement between the enthalpy and entropy values for oxazepam and lorazepam may be explained by their close structural relationship. However, the methyl group with its electron donating properties

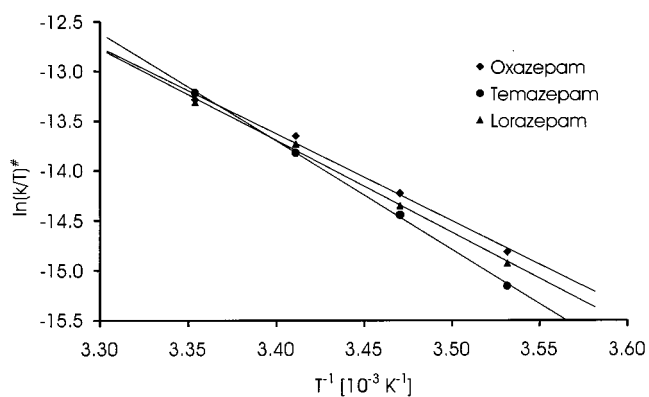


Figure 8. Eyring plot of the simulated apparent rate constant, k_f^{app} , of enantiomerization of oxazepam, temazepam, and lorazepam.

in position 1 in temazepam seems to influence the interconversion in regard to ΔH^\ddagger and ΔS^\ddagger .

In principle, the calculated rate constant also allows the determination of the enantiomeric excess (*ee*) of nonracemic samples before separation even if the enantiomers are interconverting during the time scale of partitioning. Figure 9 displays the simulated chromatogram of the pure enantiomer A, interconverting at a rate constant of $k_{-1}^{\text{app}} = 3.15 \times 10^{-4} \text{ s}^{-1}$ (data from example 3 in Table 1).

(28) Sandström, J. *Dynamic NMR Spectroscopy*; Academic Press: London, 1982; 111–112.

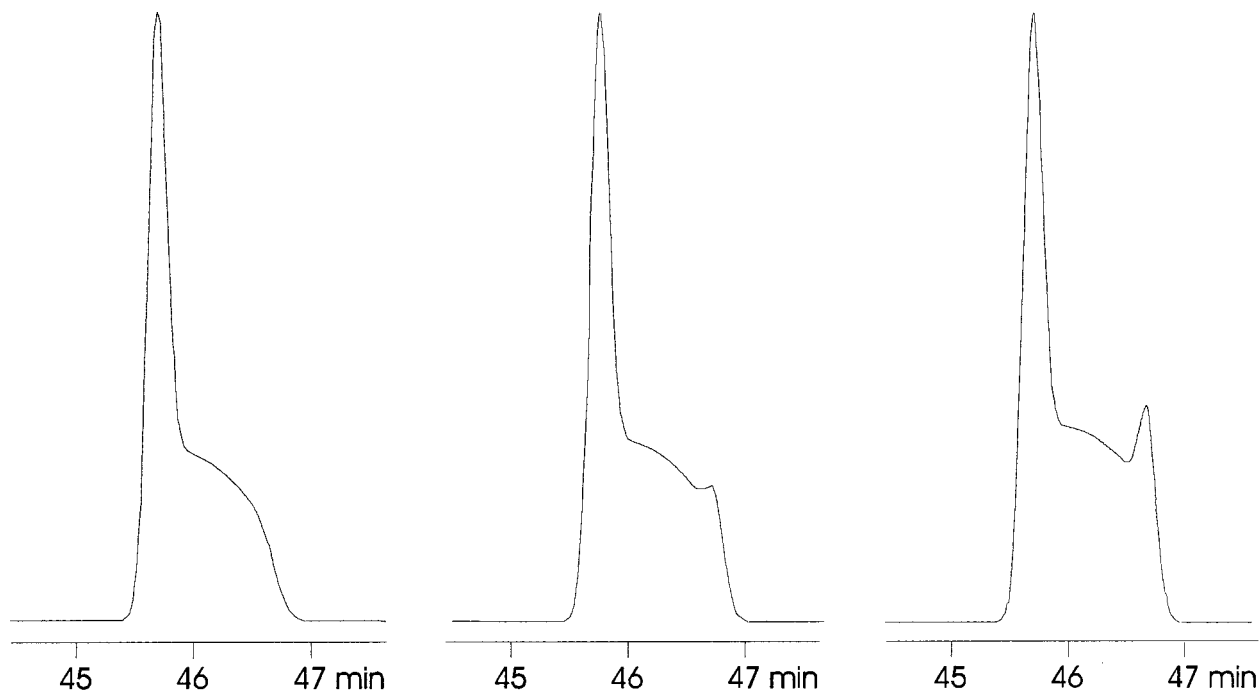


Figure 9. Simulated chromatograms of the first eluted enantiomer of oxazepam with an enantiomeric excess (ee) of 100% (left), 80% (middle), and 60% (right) (data from example 3 in Table 1) with interconversion taking place during the separation process.

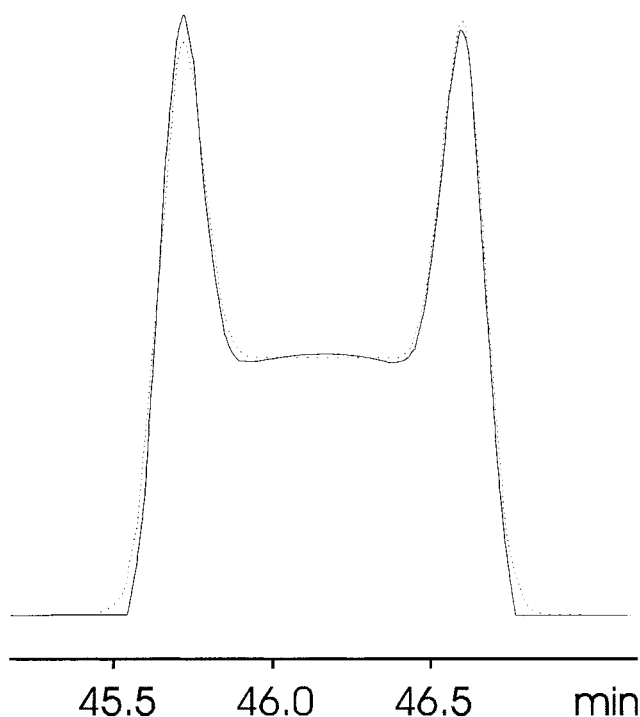


Figure 10. Comparison of simulations obtained by the modified stochastic model (dotted line) and the theoretical plate model (plain line) (data from example 3 in Table 1). The differences of the two chromatograms arise from the different plate numbers used for simulation. For the theoretical plate model the average of the mean plate numbers was used, whereas true mean plate numbers were used for the stochastic model.

Applicability to One-Phase Systems. As demonstrated in Figure 10, both the theoretical plate model and the stochastic model yield essentially the same simulated chromatograms. Thus, although both models have been derived for chromatographic two-phase systems, the obtained results demonstrate that both models

are compatible with a one-phase system involving partitioning equilibria in a micelle (DMEKC).

An explanation for this phenomenon is the existence of a pseudo-stationary phase, as already proposed by Terabe et al.,²³ which serves as an interphase within the one-phase system and is therefore comparable to a CSP in an ordinary enantiomeric separation.

Accuracy and Precision. The determined enantiomerization barriers ΔG^\ddagger of oxazepam compare well with data previously reported from independent methods,^{12,29,34} e.g., DHPLC,¹² polarimetry,^{27,33} and the investigation of the racemization kinetics of hydrolysis of optically pure salts,²⁹ provided the difference between the terms enantiomerization and racemization is considered.^{3,12} A comparison of the enantiomerization barriers of benzodiazepines obtained by other methods described in the literature is given in Table 3. As the data compare well to those determined, the accuracy and applicability of the present approach employed in a chromatographic one-phase system based on electromigration (DMEKC) is demonstrated.

The precision of the DMEKC experiment was determined as follows. The enantiomerization of all three benzodiazepines was repeated at least 5 times at exactly the same experimental conditions. The repeatability of the method is quite satisfactory (2.93σ (standard deviation); error of $\Delta G^\ddagger(19^\circ\text{C}) = 0.41 \text{ kJ}\cdot\text{mol}^{-1}$ at 10°C). The precision of the enantiomerization experiment was then rechecked after 6 months with an identical system, but a

(29) Yang, S. K. *Enantiomer* **1998**, *3*, 485–490.

(30) Barret, J.; Franklyn Smyth, W.; Davidson, I. E. *J. Pharm. Pharmacol.* **1972**, *25*, 387–393.

(31) Yang, S. K.; Lu, X.-L. *Chirality* **1992**, *4*, 443–446.

(32) Yang, S. K.; Tank, R.; Pu, Q.-L. *J. Labelled Compd. Radiopharm.* **1996**, *38*, 753–759.

(33) Yang, S. K. *Chirality* **1999**, *11*, 179–186.

(34) Yang, T. J.; Yang, S. K. *J. Food Drug Anal.* **1995**, *3*, 173–183.

new capillary. Within the given errors the same enantiomerization barriers as previously observed were determined.

CONCLUSION

DMEKC represents a useful tool for the measurement of enantiomerization barriers under physiological conditions. This is an advantage compared with DHPLC, which frequently uses a large amount of organic solvents or aqueous systems containing organic modifiers. In contrast to classical enantiomerization studies, the method described does not require enantiomerically enriched material or even the pure enantiomers.

The temperature applied is only limited by the boiling and freezing points of the buffer solution and the solubility of the chiral surfactant. The flexible temperature range from -10 to $+80$ °C allows the determination of enantiomerization barriers, ΔG^\ddagger ,

between 80 and 120 kJ mol⁻¹. The temperature constancy throughout each run, achieved through efficient thermostating, permits the use of high ionic strength running buffers and thus helps to improve peak resolution.

ACKNOWLEDGMENT

This work was supported by the Deutsche Forschungsgemeinschaft, Fonds der Chemischen Industrie and the Graduiertenkolleg "Chemistry in Interphases". O.T. thanks the Stiftung Stipendien-Fonds der Chemischen Industrie for a doctorate scholarship.

Received for review December 15, 1999. Accepted March 20, 2000.

AC991439G